*J. Indian Inst. Sci.*, May–June 1996, 76, 379–387.


# Steady simple shear flow past a circular cylinder at moderate and high Reynolds numbers—A numerical study

C. V. RAGHAVARAO AND Y. V. S. S. SANYASIRAJU
Department of Mathematics, Indian Institute of Technology, Madras 600 036, India.

Received on August 25, 1994; Revised on October 16, 1995.

**Abstract**

Steady, viscous, incompressible flow past a circular cylinder, placed symmetrically in a simple shear field, has been studied numerically using the upwind finite-difference method at moderate and high Reynolds numbers up to 500. The present results are in good agreement with the theoretical and numerical results which are available at small and moderate Reynolds numbers. Unlike the flow at moderate Reynolds numbers up to Re = 70, here a vortex is formed near the surface of the cylinder which grows in size as the Reynolds number increases. The separation of the flow on the surface of the cylinder is also observed.

**Keywords:** Shear flow, circular cylinder, numerical study, fluid dynamics.

## 1. Introduction

Two-dimensional, steady, viscous, incompressible flow past a circular cylinder is one of the classical problems in fluid dynamics. Many authors studied both uniform and non-uniform flow fields at large distances from bodies like circular cylinders and spheres. Among these, Bretherton[1], who studied a combination of uniform flow and a simple shear flow at large distances, and Robertson *et al.*[2], by taking a uniform shear flow at large distances, have initially theoretically investigated at small Reynolds numbers. Later, Kossack and Acrivos[3] studied numerically the uniform shear flow past a circular cylinder up to Reynolds number Re = 70. The main observations of the above investigations are that the flow is not separated from the surface of the cylinder even at Re = 70. But the closed streamlines around the body which are observed for creeping flow and inviscid flow disappear as Re increases to 70. Also the wake region comes closer and closer to the surface of the body as Re increases.

We consider the two-dimensional, steady, viscous, incompressible flow past a circular cylinder at high Reynolds numbers, when the velocity at large distances is described by a simple shear. Here, we assume that the cylinder is placed symmetrically in the shear field so that the lift and drag are identically zero. Also the cylinder is allowed to rotate freely so that the dimensionless torque vanishes.

## 2. Formulation of the problem

The schematic picture of the problem considered is given in Fig. 1, with a circular cylinder of radius $a$, which is placed symmetrically in a simple shear flow with the velocity curvature denoted by $G$, a constant. The Reynolds number Re is defined as $\mathrm{Re} = Ga^2/\nu$, where $\nu$ is the coefficient of kinematic viscosity, $a$, the characteristic length (radius of the cylinder in the present case) and $Ga$, the characteristic velocity. The velocity components at sufficiently large distances for simple shear flow are given by

$$\left.\begin{aligned} u' &= \frac{\partial \psi'}{\partial y'} = Gy', \\ v' &= \frac{\partial \psi'}{\partial x'} = 0, \end{aligned}\right\} \tag{1}$$

where $\psi$ is the stream function and the prime denotes the dimensional quantities. All quantities are nondimensionalized using

$$r = \frac{r'}{a}, \quad u = \frac{u'}{Ga}, \quad \psi = \frac{\psi'}{Ga^2}.$$

Then the governing differential equations for the flow in stream function–vorticity formulation are the nonlinear Navier–Stokes equations in the nondimensional form

$$\nabla^4 \psi = -\frac{\mathrm{Re}}{r} \frac{\partial(\psi, \nabla^2 \psi)}{\partial(r, \theta)} \tag{2}$$

which is re-written as two second-order coupled equations in the form

$$\left.\begin{aligned} \nabla^2 \psi &= -\omega \\ \nabla^2 \omega &= -\frac{\mathrm{Re}}{r} \frac{\partial(\psi, \omega)}{\partial(r, \theta)} \end{aligned}\right\} \tag{3}$$

where $\nabla^2 = \dfrac{\partial^2}{\partial r^2} + \dfrac{1}{r}\dfrac{\partial}{\partial r} + \dfrac{1}{r^2}\dfrac{\partial^2}{\partial \theta^2}$.

$$v_r = \frac{1}{r}\frac{\partial \psi}{\partial \theta}, \quad v_\theta = -\frac{\partial \psi}{\partial r}, \quad \frac{\partial(u, v)}{\partial(x, y)} = \begin{vmatrix} u_x & v_x \\ u_y & v_y \end{vmatrix}.$$

The boundary conditions are

$$\left.\begin{aligned} &\psi = 0, \ \frac{\partial \psi}{\partial r} = \Omega \ \text{ on } \ r = 1 \\ &\psi = \frac{1}{2} r^2 \sin^2\theta \ \text{ as } \ r \to \infty, \\ &\omega = -1 \qquad\quad \text{as } \ r \to \infty, \end{aligned}\right\} \tag{4}$$

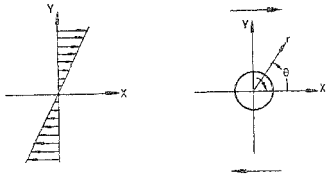


FIG. 1. The simple shear flow and the location of the cylinder.

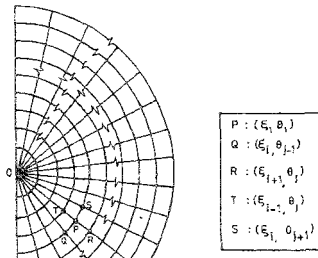


FIG. 2. Finite difference grid

where $\Omega$ is the dimensionless speed with which the cylinder rotates and $\omega$ is vorticity. The condition for vorticity $\omega$ on the surface of the cylinder is deduced using the definition of $\omega$ and $\frac{\partial \psi}{\partial r} = \Omega$. The periodicity condition is

$$\{\psi(r,\theta), \omega(r,\theta)\} = \{\psi(r,\pi+\theta)\ \omega(r,\pi+\theta)\} \tag{5}$$

which arises from the symmetry of the flow. Here $r$ and $\theta$ are the conventional cylindrical polar co-ordinates, with $\theta$ increasing in counter clockwise direction as shown in Fig. 1. Because of the symmetry of the flow half of the domain, *i.e.*, $\left(-\frac{\pi}{2}, \frac{\pi}{2}\right)$ is only considered in the numerical approximation. It is convenient to consider the problem in terms of a perturbation from the flow at large distances from the cylinder surface by taking

$$\left.\begin{aligned} \hat{\psi} &= \psi - \frac{1}{2} r^2 \sin^2\theta \\ \hat{\omega} &= \omega + 1 \end{aligned}\right\}. \tag{6}$$

Then the governing differential equations (3) and boundary conditions (4) will take the form

$$\left.\begin{aligned} \nabla^2 \hat{\psi} &= -\hat{\omega} \\ \nabla^2 \hat{\omega} &= -\frac{\mathrm{Re}}{r} \frac{\partial(\hat{\psi}, \hat{\omega})}{\partial(r,\theta)} - \mathrm{Re}\left[\sin^2\theta \frac{\partial \hat{\omega}}{\partial \theta} - r \sin\theta \cos\theta \frac{\partial \hat{\omega}}{\partial r}\right] \end{aligned}\right\} \tag{7}$$

where $\nabla^2$ defines as in eqn (3).

$$\left.\begin{aligned} &\hat{\psi} = -\frac{1}{2}\sin^2\theta \\ &\frac{\partial\hat{\psi}}{\partial r} = \Omega - \sin^2\theta \end{aligned}\right\} \text{ at } r = 1 \\ \hat{\psi} = 0,\ \hat{\omega} = 0 \text{ as } r \to \infty \Bigg\}. \tag{8}$$

## 3. Numerical approximation

The governing coupled differential equations are solved numerically using the upwind finite-difference scheme. The stream function $\hat{\psi}$ and $\hat{\omega}$ vary rapidly near the cylinder surface and hence a smaller step size is essential in this region of the flow field. Far away from this surface larger step sizes are permissible. To meet this requirement, the independent variables $r$ and $\theta$ are transformed as

$$r = e^{\pi\xi} \text{ and } \theta = \pi\eta.$$

With these transformations the governing differential equations (7) and the boundary conditions (8) take the form

$$\left.\begin{aligned} &\nabla^2\hat{\psi} = -\pi^2 e^{2\pi\xi}\hat{\omega} \\ &\nabla^2\hat{\omega} = -\mathrm{Re}\frac{\partial(\hat{\psi},\hat{\omega})}{\partial(\xi,\eta)} - \mathrm{Re}\,\pi e^{2\pi\xi}\sin\pi\eta\left[\sin\pi\eta\frac{\partial\hat{\omega}}{\partial\eta} - \cos\pi\eta\frac{\partial\hat{\omega}}{\partial\xi}\right] \end{aligned}\right\}. \tag{9}$$

where $\nabla^2 = \dfrac{\partial^2}{\partial\xi^2} + \dfrac{\partial^2}{\partial\eta^2}$

$$\left.\begin{aligned} &\hat{\psi} = -\frac{1}{2}\sin^2\pi\eta \\ &\frac{\partial\hat{\psi}}{\partial\xi} = \Omega - \sin^2\pi\eta \end{aligned}\right\} \text{ at } \xi = 0 \\ \hat{\psi} = 0, \hat{\omega} = 0 \text{ as } \xi \to \xi_\infty \Bigg\}. \tag{10}$$

The condition on the surface of the cylinder for vorticity comes from the relation of $\partial\hat{\psi}/\partial\xi$ and the definition of $\hat{\omega}$. By fixing the outer boundary $\xi_\infty$ at $\xi_\infty = .954$, the boundary condition on $\hat{\psi}$ at $\xi_\infty$ is modified[3] as

$$\hat{\psi} = A + B\pi\xi_\infty$$

where $A = -\displaystyle\int_0^\infty g\ln(t)\,dt - \frac{1}{4}$ and $B = \Omega - \frac{1}{2} + \displaystyle\int_0^\infty g(t)\,dt$

with $g(r) = -\frac{r}{\pi}\int_{-\pi/2}^{\pi/2} \hat{\omega}(r,\theta)\, d\theta$.

The finite-difference discretization of the $\xi$–$\eta$ domain is given in Fig. 2. The nodal points are the points of intersection of $\xi$ = constant (circles) and $\eta$ = constant (lines). The second-order derivatives in eqn (9) are approximated by central differences of order $\Delta\xi^2$ or $\Delta\eta^2$, where $\Delta\xi$ and $\Delta\eta$ are the step lengths in $\xi$ and $\eta$ directions, respectively. The nonlinear terms in the coupled equations are approximated with first-order upwind differences of the form

$$(fF)_\xi = .5(f - |f|)F_{i+1,j} + |f|F_{i,j} - .5[f + |f|]F_{i-1,j}$$

where $f$ is $\partial\hat{\psi}/\partial\xi$ or $\partial\hat{\psi}/\partial\eta$ which is approximated with central differences at any point $(\xi_i, \eta_j)$ and $F$ is the vorticity $\hat{\omega}$. The boundary condition on the surface of the cylinder is taken as

$$\hat{\omega}_{0,j} = -\frac{8\hat{\psi}_{1,j} - \hat{\psi}_{2,j} + 3.5\sin^2\pi\eta - 6\Delta\xi\left[\Omega - \pi\sin^2\pi\eta\right]}{2\pi^2(\Delta\xi)^2} \tag{11}$$

where $j$ is the node number in $\eta$ direction and 0, 1 and 2 are the nodes in $\xi$ direction.

The Block SLOR method is used in the iteration process. The resulting algebraic equations are solved using a tridiagonal solver along each line. The basic steps in the iteration process are

(i) $\Omega$ is approximated using zero torque relation[3] $T = -\frac{2\pi}{\mathrm{Re}}\left\{2\left[\Omega - \frac{1}{2}\right] + \int_0^1 \hat{\omega}(0,\eta)\, d\eta\right\}$.

(ii) Vorticity on the body is calculated using $\Omega$ and eqn (11).

(iii) $\hat{\omega}$ and $\hat{\psi}$ are calculated along $\eta$ = constant lines using tridiagonal solver on each line. Here the two blocks $\eta = -.5$ and $\eta = .5$ are solved separately using the periodicity conditions (5) for both $\hat{\psi}$ and $\hat{\omega}$.

The above three steps are continued until the relation $|F^{(n+1)} - F^{(n)}| \le 10^{-4}$ satisfies at all inner grid points, where $n$ is the iteration number and $F$, one of the field variables, $\hat{\psi}$ and $\hat{\omega}$. This iteration process requires three under-relaxation parameters, respectively, for $\hat{\psi}$, $\hat{\omega}$ and $\Omega$. It is found that .3 and .4 are optimum for $\hat{\psi}$ and $\hat{\omega}$, respectively. For $\Omega$, a very small relaxation parameter, say .05, is required in the iteration process.

The diagonal dominance is assured because of the upwind difference approximation for the nonlinear terms even at high Reynolds numbers. To minimize the oscillations of the solution in the convergence process it is necessary to use some initial solution in the iteration process. Here we used the inviscid flow solution to solve the coupled equations at small Reynolds numbers, say at Re = .047, and this solution is used as the starting solution at next higher Reynolds numbers and so on.

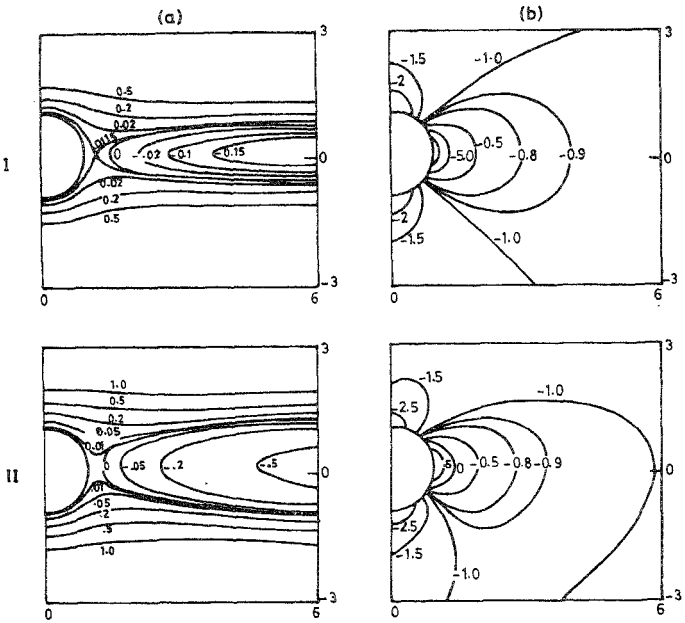


FIG. 3.a. Streamliness, b. equi-vorticity lines (I) Re = 0.047, (II) Re = 1.0.

The calculations were carried out on the Siemens BS2000 mainframe at the Indian Institute of Technology, Madras, India, and the graphs were drawn on a PC using a software package developed by the authors. For a typical Reynolds number, say 500 with $51 \times 51$ grid, the present code required 250 seconds of CPU time.

## 4. Discussion

Using the numerical technique described above, eqns (9) along with boundary conditions are solved at Reynolds numbers of .047, 1, 10, 70, 200 and 500. As expected, the effect of the dimensionless speed $\Omega$ on the surface vorticity decreases with increasing Reynolds number. At Re = 500 the value of $\Omega$ obtained in the iteration process is .05. The corres ponding dimensionless torque is of the order of $10^{-3}$. The present results are expressed in terms of streamlines and equi-vorticity lines. To test the accuracy of the computer code developed, the results at low and moderate Reynolds numbers, *i.e.*, the corresponding

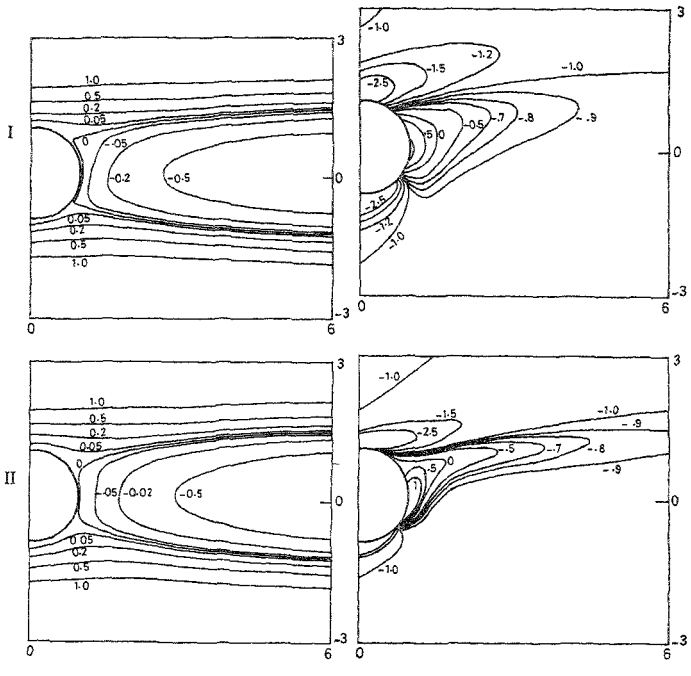


FIG. 4.a. Streamliness, b. equi-vorticity lines (I) Re = 10.0 (II) Re = 70.0

streamlines and equi-vorticity lines are presented at Re = .047 and 1 in Fig. 3 and at Re = 10 and 70 in Fig. 4, respectively. These figures show that the present results are in excellent agreement with the results of Kossack and Acrivos[3], particularly the equi-vorticity contours, which are drawn with the same scaling except for the minimum and maximum values in $y$-direction which are $-3$ to 3 instead of $-2.5$ to 2.5. The streamlines and equi-vorticity lines at higher Re, *i.e.*, at 200 and 500 are given in Fig. 5. The main difference of these flow patterns at high Reynolds numbers is the separation of the flow on the surface of the circular cylinder, which is not seen at low Reynolds numbers. This is as expected because the zero streamline comes close to the surface of the

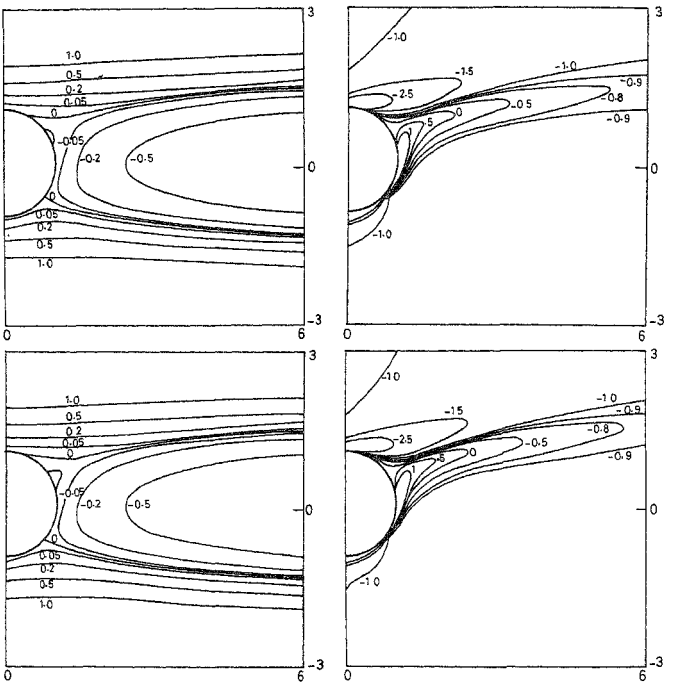


FIG. 5.a. Streamlines, b. equi-vorticity lines; (I) Re = 200.0, (II) Re = 500.0.

body as Reynolds number increases from .047 to 70, both in literature and the present results. As seen from the graphs the separation angle is increasing with the Reynolds number. The corresponding separation angles are tabulated in Table I.

**Table I**
**Separation angles as a function of Re**

| Re | 200 | 500 |
|---|---|---|
| Top sep. angle | 62.5° | 70° |
| Bottom sep. angle | −38° | −41° |

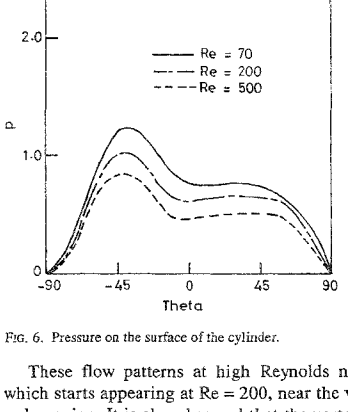


FIG. 6. Pressure on the surface of the cylinder.

These flow patterns at high Reynolds numbers reveal the formation of a vortex, which starts appearing at Re = 200, near the vicinity of the circular cylinder in the open wake region. It is also observed that the vortex so obtained at Re = 200 increases in size as Reynolds number increases from 200 to 500.

The most significant difference of the high Reynolds number flows is brought out by the corresponding pressure profiles on the surface of the cylinder. The dimensionless pressure relative to that at $\theta = \pi/2$ (*i.e.*, relative pressure divided by $\rho G^2 a^2$, $\rho$ being the density) is plotted in Fig. 6 as a function of $\theta$. It is interesting to observe from Fig. 6 that the pressure distribution on the surface of the cylinder decreases as Re increases for all $\theta$.

## 5. Conclusion

The complex problem of two-dimensional, viscous, incompressible, simple shear flow past a circular cylinder has been studied numerically at moderate and high Reynolds numbers. The main observations of the present study are:

(i) Separation of flow on the surface of the cylinder.

(ii) Formation of vortex near the surface of the cylinder in the open wake region.

## References

1. BRETHERTON, F. P. — Slow viscous motion round a cylinder in a simple shear, *J. Fluid. Mech.*, 1962, **12**, 591–613.

2. ROBERTSON, C. R. AND ACRIVOS, A. — Low Reynolds number shear flow past a rotating circular cylinder. Part 1—momentum transfer, *J. Fluid Mech.*, 1970, **40**, 685–704.

3. KOSSACK, C. A. AND ACRIVOS, A. — Steady simple shear flow past a circular cylinder at moderate Reynolds numbers: A numerical study, *J. Fluid Mech.*, 1974, **66**, 353–376.